

Observation of a Strongly Isospin-Mixed Doublet in ^{26}Si via β -Delayed Two-Proton Decay of ^{26}P

J. J. Liu (刘嘉健)¹, X. X. Xu (徐新星)^{1,2,3,4,5,*}, L. J. Sun (孙立杰)^{6,7,†}, C. X. Yuan (袁岑溪)⁸, K. Kaneko (金子也和)⁹, Y. Sun (孙扬)^{6,1,3}, P. F. Liang (梁鹏飞)², H. Y. Wu (吴鸿毅)¹⁰, G. Z. Shi (石国柱)¹, C. J. Lin (林承键)^{3,11}, J. Lee (李晓菁)², S. M. Wang (王思敏)^{12,13}, C. Qi (齐冲)¹⁴, J. G. Li (李健国)¹, H. H. Li (李红蕙)¹, Latsamy Xayavong¹⁵, Z. H. Li (李智焕)¹⁰, P. J. Li (李朋杰)¹, Y. Y. Yang (杨彦云)¹, H. Jian (简豪)¹, Y. F. Gao (高雨枫)^{1,4}, R. Fan (范锐)^{1,4}, S. X. Zha (查思贤)^{1,4}, F. C. Dai (戴凡超)^{1,4}, H. F. Zhu (朱浩钊)^{1,4}, J. H. Li (李金海)^{1,4}, Z. F. Chang (常志芳)^{1,4}, S. L. Qin (覃淑炼)^{1,4}, Z. Z. Zhang (张朝展)⁸, B. S. Cai (蔡博帅)⁸, R. F. Chen (陈若富)¹, J. S. Wang (王建松)^{16,1}, D. X. Wang (王东玺)³, K. Wang (王康)^{1,17}, F. F. Duan (段芳芳)^{1,18}, Y. H. Lam (蓝乙华)^{1,4}, P. Ma (马朋)¹, Z. H. Gao (高志浩)^{1,18}, Q. Hu (胡强)¹, Z. Bai (白真)¹, J. B. Ma (马军兵)¹, J. G. Wang (王建国)¹, C. G. Wu (武晨光)¹⁰, D. W. Luo (罗迪雯)¹⁰, Y. Jiang (蒋颖)¹⁰, Y. Liu (刘洋)¹⁰, D. S. Hou (侯东升)^{1,4}, R. Li (李忍)^{1,4}, N. R. Ma (马南茹)³, W. H. Ma (马维虎)^{1,12}, G. M. Yu (余功明)^{1,19}, D. Patel^{1,20}, S. Y. Jin (金树亚)^{1,4}, Y. F. Wang (王煜峰)^{1,21}, Y. C. Yu (余悦超)^{1,21}, L. Y. Hu (胡力元)¹⁹, X. Wang (王翔)¹⁰, H. L. Zang (臧宏亮)¹⁰, K. L. Wang (王凯龙)¹, B. Ding (丁兵)¹, Q. Q. Zhao (赵青青)², L. Yang (杨磊)³, P. W. Wen (温培威)³, F. Yang (杨峰)³, H. M. Jia (贾会明)³, G. L. Zhang (张高龙)²², M. Pan (潘敏)^{22,3}, X. Y. Wang (汪小雨)²², H. H. Sun (孙浩瀚)³, H. S. Xu (徐瑚珊)^{1,4,5}, X. H. Zhou (周小红)^{1,4,5}, Y. H. Zhang (张玉虎)^{1,4,5}, Z. G. Hu (胡正国)^{1,4,5}, M. Wang (王猛)^{1,4,5}, M. L. Liu (柳敏良)¹, H. J. Ong (王惠仁)^{1,23} and W. Q. Yang (杨维青)¹

(RIBLL Collaboration)

¹CAS Key Laboratory of High Precision Nuclear Spectroscopy, Institute of Modern Physics, Chinese Academy of Sciences, Lanzhou 730000, China

²Department of Physics, The University of Hong Kong, Hong Kong, China

³Department of Nuclear Physics, China Institute of Atomic Energy, Beijing 102413, China

⁴School of Nuclear Science and Technology, University of Chinese Academy of Sciences, Beijing 100049, China

⁵Advanced Energy Science and Technology Guangdong Laboratory, Huizhou 516003, China

⁶School of Physics and Astronomy, Shanghai Jiao Tong University, Shanghai 200240, China

⁷National Superconducting Cyclotron Laboratory, Michigan State University, East Lansing, Michigan 48824, USA

⁸Sino-French Institute of Nuclear Engineering and Technology, Sun Yat-Sen University, Zhuhai 519082, China

⁹Department of Physics, Kyushu Sangyo University, Fukuoka 813-8503, Japan

¹⁰State Key Laboratory of Nuclear Physics and Technology, School of Physics, Peking University, Beijing 100871, China

¹¹College of Physics and Technology & Guangxi Key Laboratory of Nuclear Physics and Technology, Guangxi Normal University, Guilin 541004, China

¹²Key Laboratory of Nuclear Physics and Ion-beam Application (MOE), Institute of Modern Physics, Fudan University, Shanghai 200433, China

¹³Shanghai Research Center for Theoretical Nuclear Physics, NSFC and Fudan University, Shanghai 200438, China

¹⁴KTH Royal Institute of Technology, SE-100 44, Stockholm, Sweden

¹⁵Department of Physics, Faculty of Natural Sciences, National University of Laos, Vientiane 01080, Laos

¹⁶College of Science, Huzhou University, Huzhou 313000, China

¹⁷Shanghai Institute of Applied Physics, Chinese Academy of Sciences, Shanghai 201800, China

¹⁸School of Nuclear Science and Technology, Lanzhou University, Lanzhou 730000, China


¹⁹Fundamental Science on Nuclear Safety and Simulation Technology Laboratory, Harbin Engineering University, Harbin 150001, China

²⁰Department of Physics, Sardar Vallabhbhai National Institute of Technology, Surat 395007, India

²¹School of Physics and Astronomy, Yunnan University, Kunming 650091, China

²²School of Physics, Beihang University, Beijing 100191, China

²³RCNP, Osaka University, Osaka 567-0047, Japan

 (Received 31 July 2022; revised 10 October 2022; accepted 3 November 2022; published 8 December 2022)

β decay of proton-rich nuclei plays an important role in exploring isospin mixing. The β decay of ^{26}P at the proton drip line is studied using double-sided silicon strip detectors operating in conjunction with high-purity germanium detectors. The $T = 2$ isobaric analog state (IAS) at 13 055 keV and two new high-lying states at 13 380 and 11 912 keV in ^{26}Si are unambiguously identified through β -delayed two-proton

emission ($\beta 2p$). Angular correlations of two protons emitted from ^{26}Si excited states populated by ^{26}P β decay are measured, which suggests that the two protons are emitted mainly sequentially. We report the first observation of a strongly isospin-mixed doublet that deexcites mainly via two-proton decay. The isospin mixing matrix element between the ^{26}Si IAS and the nearby 13 380-keV state is determined to be 130(21) keV, and this result represents the strongest mixing, highest excitation energy, and largest level spacing of a doublet ever observed in β -decay experiments.

DOI: [10.1103/PhysRevLett.129.242502](https://doi.org/10.1103/PhysRevLett.129.242502)

The concept of isospin was introduced by Heisenberg based on similar properties between protons and neutrons with respect to the strong interaction [1]. The proton and the neutron could be described as two isospin projections of the identical particle [2]. However, isospin symmetry is not strictly conserved, which is mainly due to proton-neutron mass difference, Coulomb interaction, and charge-dependent parts of nuclear force. Isospin symmetry breaking has been shown to be a sensitive probe of isospin non-conserving interactions and allows for precision tests of the standard model description of electroweak interactions [3].

β decay is a process of the exchange between a proton and a neutron, which offers experimental observables sensitive to isospin. Although isospin symmetry requires the entire transition strength to be concentrated on one single isobaric analog state populated by the superallowed Fermi β decay, the Fermi strength splitting between the isobaric analog state (IAS) and a neighboring state with the same spin and parity via strong isospin mixing has been observed in the β decays of $^{31}\text{Cl} \rightarrow ^{31}\text{S}$ [4], $^{37}\text{Ca} \rightarrow ^{37}\text{K}$ [5], $^{55}\text{Cu} \rightarrow ^{55}\text{Ni}$ [6], and $^{56}\text{Zn} \rightarrow ^{56}\text{Cu}$ [7]. The fragmentation of the Fermi strength is a striking feature of isospin symmetry breaking, providing a direct measurement of the isospin mixing matrix element and the amount of isospin impurity. In those four cases, the isospin-mixed doublets were determined via the observation of either $\beta\gamma$ or βp . The observation of the isospin-forbidden p and $2p$ emissions from the ^{26}Si IAS in the β decay of ^{26}P [8] is a signature of isospin symmetry breaking. The large Q_β value of ^{26}P allows us to expand the exploration of the Fermi strength splitting into excitation energies above 10 MeV.

So far, of 13 identified $\beta 2p$ precursors [9–12], only in several cases [13–17] have the proton-proton correlations been studied to investigate the mechanism of $2p$ emission. A recent β -decay study of ^{27}S revealed that the mechanism of $2p$ emission from the ^{27}P IAS to the ground state of ^{25}Al is sequential by employing a state-of-the-art silicon array [18]. The β decay of ^{26}P has been one of the most studied cases, yet the mechanism of $2p$ emission, either direct emission or sequential emission, is still not clear. In this Letter, we present the detailed study of β -delayed two-proton decay of ^{26}P and the first observation of a strongly isospin-mixed doublet in ^{26}Si .

The β -decay experiment of ^{26}P [19] was performed at the Heavy Ion Research Facility in Lanzhou (HIRFL) [20]. The

experimental details were described in Refs. [18,19,21,22] and is briefly repeated here for completeness. The nuclei of interest were produced via the projectile fragmentation of a 80.6-MeV/nucleon $^{32}\text{S}^{16+}$ primary beam impinging on a 1581- μm -thick ^9Be target. The projectile fragments were separated and purified using the Radioactive Ion Beam Line in Lanzhou (RIBLL1) [23]. The ions in the secondary beam were identified by using the energy loss and time of flight obtained with two quadrant silicon detectors (QSDs) and two plastic scintillators, respectively. The identified ions were implanted into a silicon array consisting of three W1-type double-sided silicon strip detectors (DSSDs) with thicknesses of 142 (DSSD1), 40 (DSSD2), and 304 μm (DSSD3) for measuring the position and energy of charged particles. Previously known decay branches from nearby nuclides were observed using the same detection setup in the same campaign, providing energy and detection efficiency calibration standards [18,22,24]. Three quadrant silicon detectors, QSD1 (1546 μm), QSD2 (300 μm), and QSD3 (300 μm) were installed downstream to measure β particles and to veto light-particle contaminants in the secondary beam. γ rays were detected by five Clover-type high-purity germanium detectors surrounding the silicon array.

The β -decay half-life ($T_{1/2}$) of ^{26}P was measured to be 43.6(3) ms by fitting the decay curve using the maximum likelihood method with an exponential function combined with a constant background [19]. Figures 1(a) and 1(b) show the charged-particle spectra measured by DSSD3 and DSSD2, respectively. A comparison of Figs. 1(a) and 1(b) shows the thinner DSSD2 has less β -summing effect than DSSD3 and can be used for distinguishing adjacent peaks and a consistency check of DSSD3. The half-life of each labeled proton peak in Figs. 1(a) and 1(b) is extracted to verify that they did in fact originate from the β -delayed proton decay of ^{26}P rather than from long-lived contaminants. In order to place the observed proton transitions in the decay scheme, we conduct a $p\gamma$ coincidence analysis. The β -delayed one- and two-proton decays to excited states in ^{25}Al and ^{24}Mg give rise to the observation of γ rays at 452, 493, 845, 945, 1338, 1612, 1789, and 1369 keV with uncertainties of around 2 keV, as shown in Fig. 1(c). The 1797-keV γ -ray peak corresponds to the transition from the 2^+ first excited state to the 0^+ ground state of ^{26}Si based on the well-studied ^{26}P β -delayed γ decay [25,26].

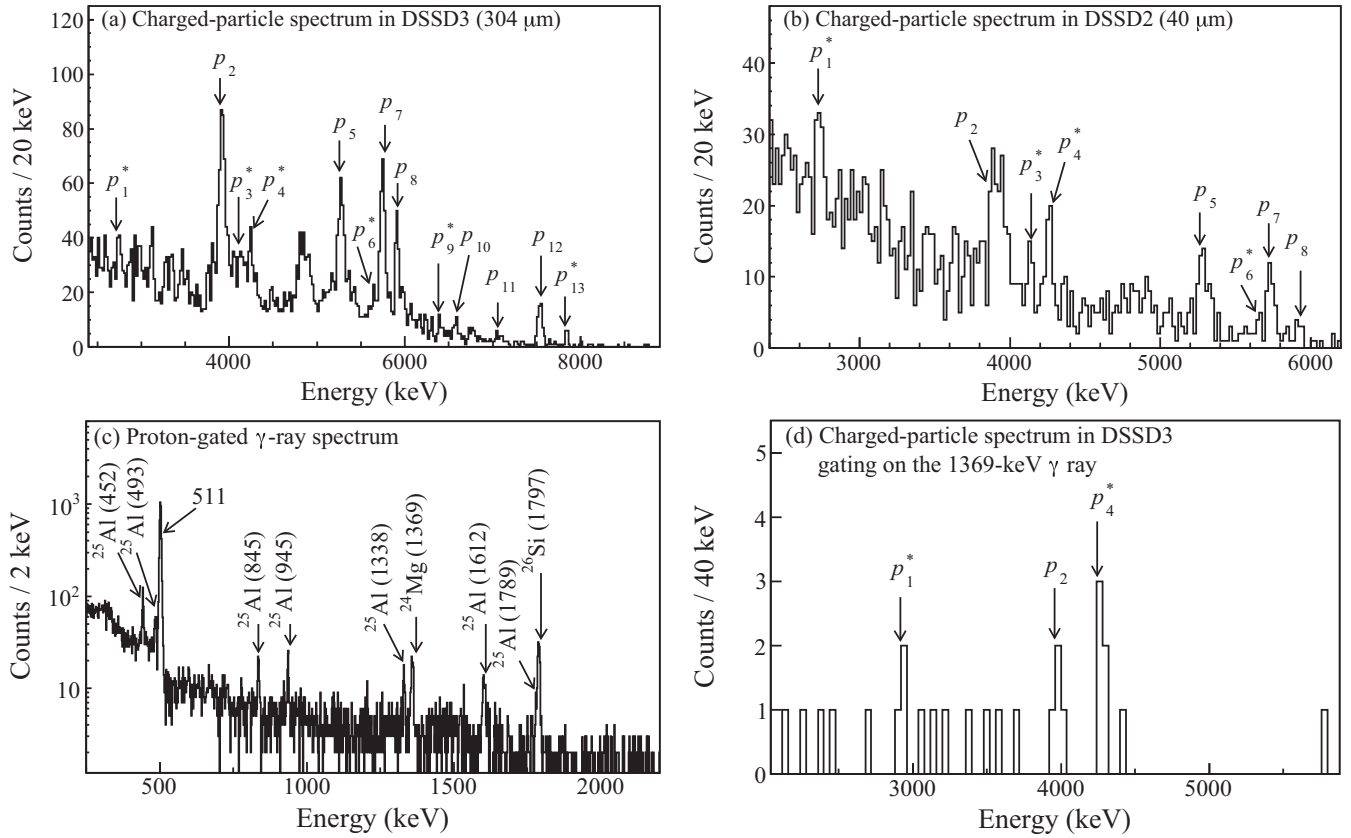


FIG. 1. Energy spectra of β -delayed protons from the decay of ^{26}P measured by (a) DSSD3 (304 μm) and (b) DSSD2 (40 μm), respectively. (c) γ -ray spectrum measured by Clover detectors in coincidence with β -delayed protons of ^{26}P in DSSD3. (d) Charged-particle spectrum acquired by DSSD3 in coincidence with the 1369-keV ^{24}Mg γ ray. Each γ peak is labeled by the emitting nucleus and its energy rounded to the closest integer in units of keV. The proton peaks labeled with an asterisk (*) are first observed in this Letter.

TABLE I. Summary of β -delayed one- and two-proton emissions in the decay of ^{26}P in this Letter, focusing on the IAS and two newly observed states. The decay energies [$E_{p/2p}$], the absolute intensities [$I_{p/2p}$], the excitation energies of the initial states [E_i] of ^{26}Si , and the excitation energies of the final states [E_f] of proton transitions are listed. The proton peaks labeled with an asterisk (*) are first observed in this Letter.

Peak	$E_{p/2p}$ (keV)	$I_{p/2p}$ (%)	E_i (keV)	E_f (keV)
Two-proton emission to ^{24}Mg				
1*	2758(7)	0.18(11)	11 912(4)	1369
2	3902(3)	0.63(22)	13 055(2) ^{IAS}	1369
3*	4125(5)	0.29(10)	11 912(4)	0
4*	4250(10)	0.72(21)	13 380(13)	1369
5	5277(4)	1.19(24)	13 055(2) ^{IAS}	0
6*	5630(20)	0.19(7)	13 380(13)	0
One-proton emission to ^{25}Al				
7	5751(3)	0.81(14)	13 055(2) ^{IAS}	1790
8	5921(4)	0.43(9)	13 055(2) ^{IAS}	1613
9*	6401(10)	0.072(57)	11 912(4)	0
10	6587(6)	0.12(2)	13 055(2) ^{IAS}	945
11	7075(16)	0.18(3)	13 055(2) ^{IAS}	452
12	7543(4)	0.29(4)	13 055(2) ^{IAS}	0
13*	7854(6)	0.07(2)	13 380(13)	0

The energies, intensities, and assignments of each proton peak are summarized in Table I. p_2 , p_5 , p_7 , p_8 , p_{10} , p_{11} , and p_{12} were previously assigned as proton emissions from the ^{26}Si IAS [8]. The two-proton peak p_2 overlaps with several one-proton peaks [8] with similar energies. p_2 is observed to be in coincidence with the 1369-keV γ ray originating from the 2^+ first excited state of ^{24}Mg as shown in Fig. 1(d). p_1 , p_3 , p_4 , p_6 , p_9 , and p_{13} are observed in ^{26}P β decay for the first time. p_1 and p_4 are observed in coincidence with the 1369-keV ^{24}Mg γ ray in Fig. 1(c), indicating that they are β -delayed two protons through two previously unknown excited states in ^{26}Si to the first excited state of ^{24}Mg . The relative energy difference indicates that these two newly observed ^{26}Si states also possibly decay by p_3 and p_6 to the ground state of ^{24}Mg and p_9 and p_{13} to the ground state of ^{25}Al . Other unlabeled proton peaks have been studied by Ref. [8].

To further confirm that p_1 – p_6 are $2p$ emissions, the proton-proton coincidence was employed based on the granularity of the silicon array [18]. This method was only applied to the implantation events in DSSD2, where the escaping two protons were detected by the adjacent DSSD1 and/or DSSD3. Therefore, the $2p$ -decay energy with an uncertainty of 100 keV should be the sum of the effective

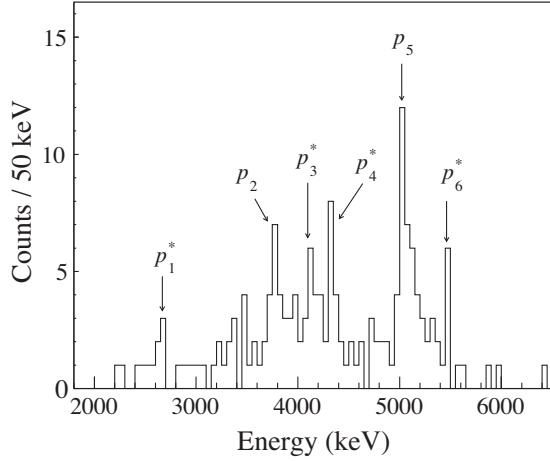


FIG. 2. Two-proton decay energy spectrum of the events, in which two protons escaped from the implantation detector DSSD2 and were detected by the adjacent DSSD1 and/or DSSD3.

energy signals from the three fired pixels of DSSDs [18]. The total energy spectrum of three fired pixels is shown in Fig. 2, where peaks at 2758, 3902, 4125, 4250, 5277, and 5630 keV are observed, confirming they are two-proton transitions.

On the other hand, to study the mechanism of the two-proton emissions from excited states of ^{26}Si , proton-proton angular correlations were extracted from the positions of the escaping two protons based on the proton-proton coincidence [18]. The measured proton-proton angular distributions of the 5277-keV $2p$ and the 3902-, 4125-, and 4250-keV combined $2p$ are shown in Figs. 3(a) and 3(b). Our Monte Carlo simulations using a schematic model [18,27–30] take into account two extreme cases: the diproton emission and the sequential emission. While the angular distribution of the diproton emission tends to have a marked peak at around 30° due to a quasibound s -singlet configuration, the sequential emission gives an approximately isotropic distribution which shows a “double hump” shape due to geometrical effects of the detector arrangements [18]. By fitting the experimental angular distribution with a normalized simulated distribution using the maximum-likelihood method [18], sequential emission with a branching ratio of 100% was obtained in Fig. 3(a), consistent with the previous study [31,32] as the diproton emission is spin-parity forbidden for the transition from the IAS of ^{26}Si to the ground state of ^{24}Mg . Similarly, Fig. 3(b) also demonstrates a dominantly sequential mechanism in the 3902-, 4125-, and 4250-keV $2p$ transitions.

Based on the one- and two-proton separation energies of ^{26}Si from the atomic mass evaluation (AME2020) [33] and the measured energies, the excitation energy of the ^{26}Si IAS was deduced to be 13 055(2) keV. Adding all the intensities of the proton branches from the IAS in ^{26}Si yields a β -feeding intensity (I_β) of 3.6(4)%, corresponding to a comparative half-life expressed in terms of logarithms $\log ft = 3.28(6)$. The mass excess of the ground state of ^{26}P

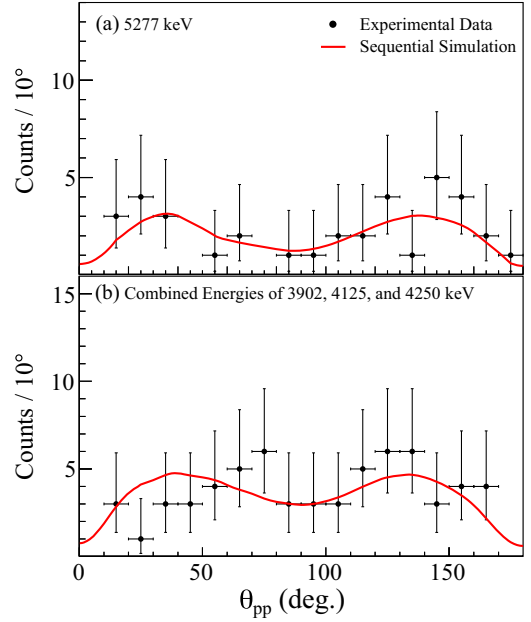


FIG. 3. Distributions of the opening angle of two protons at (a) 5277 keV and (b) combined energies of 3902, 4125, and 4250 keV in Fig. 2. The colored curves are simulation results assuming sequential emission and the black dots are experimental results in the present Letter.

can be deduced from the equation $\Delta(^{26}\text{P}) = \Delta(\text{IAS}) + \Delta E_C - \Delta_{nH}$ [34], where $\Delta(\text{IAS})$ is the mass excess of the IAS of ^{26}Si , ΔE_C is the Coulomb displacement energy between the ground state of ^{26}P and the ^{26}Si IAS determined by a semi-empirical relation in Ref. [34], and Δ_{nH} is the mass excess difference between a neutron and a hydrogen atom [33]. In this way, the atomic mass excess of ^{26}P equals 11 144(61) keV, giving a decay energy $Q_{EC} = 18285(61)$ keV. These two values are consistent with the values of 10 970(200) and 18 110(200) keV given by AME2020 [33]. Similarly, two new excited states of ^{26}Si at 13 380(13) and 11 912(4) keV with β -feeding intensities of 0.98(21)% and 0.54(16)% are determined, as shown in Fig. 4, corresponding to $\log ft$ values of 3.69(10) and 4.59(13), respectively. As commented in Ref. [35], one can distinguish the Fermi and Gamow-Teller (GT) transitions from different $\log ft$ values. The measured $\log ft$ value of the 11 912-keV state is well within the typical GT transition range of $4.0 < \log ft < 6.0$. On the other hand, the $\log ft$ values of both the IAS and the 13 380-keV state are both smaller than 3.8, which may involve a Fermi transition component and therefore requires more careful study.

The experimental $\log ft$ values for β transitions are related to the Gamow-Teller transition strengths $B(\text{GT})$ and Fermi transition strengths $B(F)$ by

$$ft = \frac{K/g_V^2}{B(F) + (g_A/g_V)^2 B(\text{GT})}, \quad (1)$$

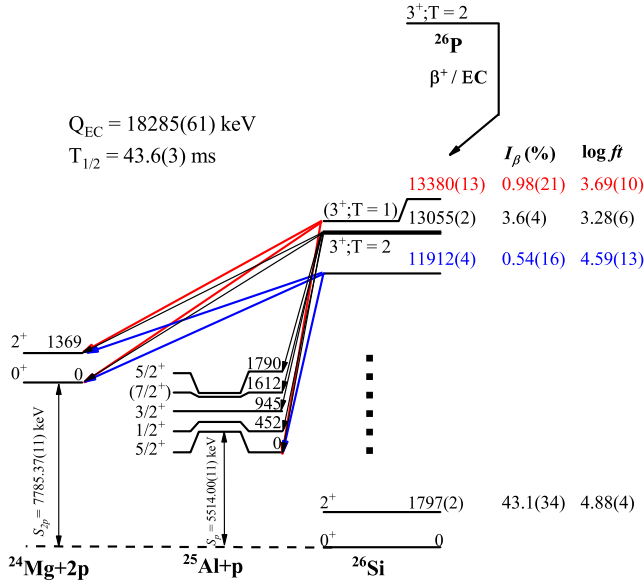


FIG. 4. Partial decay scheme of ^{26}P deduced from the present Letter. The S_p and S_{2p} of ^{26}Si are adopted from Ref. [33]. The black, blue, and red arrows represent transitions from the initial states of IAS, 11 912 keV, and 13 380 keV, respectively. The I_β and $\log ft$ value of the first excited state ($J^\pi = 2^+$) in ^{26}Si are adopted from Ref. [25].

where $K/g_V^2 = 6144.48 \pm 3.70$ s [3] and $(g_A/g_V)^2 = (-1.2756 \pm 0.0013)^2$ [36], with g_V and g_A being the free vector and axial-vector coupling constants of the weak interaction. Then the total transition strength can be defined as $B = B(F) + (g_A/g_V)^2 B(\text{GT})$.

The total Fermi transition strength for $T = 2$ ^{26}P decay should fulfill the sum rule $B(F) = |N - Z| = 4$, corresponding to a model-independent $\log ft$ value of 3.1864(3) [3,36]. However, the experimental $\log ft$ value 3.28(6) of the ^{26}Si IAS at 13 055 keV corresponds to a much smaller $B_{\text{IAS}}^{\text{exp}} = 3.2(4)$, indicating at least 0.8(4) of Fermi strength contributes to other states. On the other hand, the abnormally small $\log ft = 3.69(10)$ for the 13 380-keV state corresponds to a transition strength $B_{13\,380}^{\text{exp}} = 1.25(28)$. Such a strong transition suggests that the missing Fermi strength is mainly concentrated on this state. In this case, the IAS and the 13 380-keV state can be considered an isospin-mixed doublet.

We have performed the theoretical calculations using the shell-model code KSHELL [37] to investigate the properties of the IAS and other high-lying excited states of ^{26}Si . A total of 12 different Hamiltonians were used, including the original USD [38], USDA [39], and USDB [39], and their modified versions taking into account the empirical isospin-nonconservation (INC) [40], the weakly-bound effect (WBE) of the proton $1s_{1/2}$ orbit [41], and both of them. As a result, the smallest $\log ft$ value for the Gamow-Teller transitions was estimated to be 4.41, confirming that the 11 912-keV state with a $\log ft$ value of 4.59 is populated by

TABLE II. Summary of isospin-mixed doublets observed in β decay. Columns 2–4 report the excitation energies (E_x), observed level spacings (ΔE), and isospin mixing matrix elements (ν).

Transition	E_x (keV)	ΔE (keV)	ν (keV)
$^{26}\text{P} \rightarrow ^{26}\text{Si}$	13 380(13)	325(13)	130(21)
	13 055(2) ^{IAS}		
$^{31}\text{Cl} \rightarrow ^{31}\text{S}$ [4]	6390.2(7)	111.2(9)	41(1)
	6279.0(6) ^{IAS}		
$^{37}\text{Ca} \rightarrow ^{37}\text{K}$ [5]	5050.6 ^{IAS}	34.5	$6.9^{+0.1}_{-2.5}$
	5016.1		
$^{55}\text{Cu} \rightarrow ^{55}\text{Ni}$ [6]	4599 ^{IAS}	20	9(1)
$^{56}\text{Zn} \rightarrow ^{56}\text{Cu}$ [7]	4579	85(198)	40(23)
	3508(140) ^{IAS}		
	3423(140)		

a Gamow-Teller transition. Concentrating on the doublet of IAS and 13 380 keV, first, in two significant indications among all Hamiltonians, the $B(\text{GT})_{\text{IAS}}^{\text{theory}}$ is at least 2 orders of magnitude smaller than the $B(F)_{\text{IAS}}^{\text{theory}}$, confirming that the transition strength to the IAS contains essentially pure Fermi transition. Second, the largest calculated $B(\text{GT})^{\text{theory}} = 0.24$ among all possible states is much smaller than $B_{13\,380}^{\text{exp}} = 1.25(28)$, indicating that the 13 380-keV state is indeed dominated by a Fermi transition. Furthermore, the USDB result with a WBE modification predicts that $B(F)_{\text{IAS}}^{\text{theory}} = 2.83$ and $B(F)_{13\,380}^{\text{theory}} = 1.07$, consistent with our experimental values $B(F)_{\text{IAS}}^{\text{exp}} = 3.2(4)$ and $B(F)_{13\,380}^{\text{exp}} = 0.8(4)$, respectively. As the isospin-mixed state can be expressed by a combination of pure $|T = 2\rangle$ and $|T = 1\rangle$ with the isospin mixing angle θ , using the following formula [6,42]:

$$\begin{aligned} \tan^2 \theta &= \frac{B(F)_{13\,380}^{\text{exp}}}{B(F)_{\text{IAS}}^{\text{exp}}}, \\ \nu &= \frac{\Delta E \sin(2\theta)}{2}, \\ \varepsilon &= \Delta E \cos(2\theta), \end{aligned} \quad (2)$$

we determine the mixing angle parameter $\theta = 27(6)^\circ$, the unperturbed level spacing $\varepsilon = 195(54)$ keV, and the isospin mixing matrix element $\nu = 130(21)$ keV, taking into account the observed level spacing $\Delta E = 325(13)$ keV. It should be noted that, when extracting the ν value, we adopt a prudent approach by omitting the $B(\text{GT})_{\text{IAS}}$ component, which would reduce the extent of mixing. Nevertheless, the ν value obtained in the present Letter is still significantly larger than all previously reported values (see Table II).

The abnormally large isospin mixing matrix element between the IAS and the 13 380-keV state presents a challenge to the theoretical understanding of isospin mixing [43,44]. In addition to the isospin dependence of nuclear

and Coulomb forces, the weakly bound (or continuum) effect [41,45,46] has been found to induce isospin mixing. Our shell-model calculation using USDB with a WBE modification shows that the Fermi transition from the ^{26}P ground state to the IAS in ^{26}Si is dominated by converting a $0d_{5/2}$ proton into a $0d_{5/2}$ neutron. Because of the different asymptotic behavior of the single-particle wave function, the continuum effect between proton $1s_{1/2}$ and $0d_{5/2}$ orbitals would increase configuration mixing in ^{26}Si IAS, thus reducing the Fermi strength to the IAS and enhancing the Fermi strength splitting. Another possible explanation for strong isospin mixing may have to do with nuclear deformation [47,48]. Wang and Friedman [47] extended the discussion of MacDonald in the spherical picture [43] by calculating the mixing of isospin states in the deformed Nilsson model [49]. They concluded that deformation allows for a significant enhancement in the Coulomb mixing over what is possible with a spherical nucleus. In fact, all the nuclei involved in this Letter are predicted to be highly deformed by the finite-range droplet macroscopic and the folded-Yukawa single-particle microscopic nuclear-structure models [50].

In summary, the β -decay experiment of ^{26}P was carried out with a silicon array consisting of three DSSDs of different thicknesses and five surrounding Clover detectors at RIBLL1 of HIRFL. Two new states at 11 912 and 13 380 keV in ^{26}Si were identified in the β decay of ^{26}P . Angular correlations of two protons emitted from ^{26}Si excited states were measured to study the mechanism of $2p$ emission. The dominant component for two-proton emissions in the β decay of ^{26}P is found to be sequential based on thorough simulation-to-data comparisons. The anomaly of $\log ft$ values between the IAS and the 13 380-keV state provides clear evidence of the strong isospin mixing between the doublet in ^{26}Si . An isospin mixing matrix element of 130(21) keV is obtained, representing the strongest mixing ever observed in β -decay experiments. To have a better understanding of the nature of isospin symmetry breaking, high-precision measurements of Fermi strength splitting should be performed for more nuclides. Theoretical models should also be developed to explore the mechanism behind the unexpectedly strong isospin mixing in high-lying states with a large level spacing.

This work is supported by the Strategic Priority Research Program of Chinese Academy of Sciences under Grant No. XDB34010300, the Ministry of Science and Technology of China under National Key R&D Programs No. 2018YFA0404404 and No. 2016YFA0400503, CAS Project for Young Scientists in Basic Research No. YSBR-002, Heavy Ion Research Facility in Lanzhou (HIRFL) under Grant No. HIR2021ZD001, National Natural Science Foundation of China under Grants No. 12022501, No. 12105329, No. U1932206, No. U1632136, No. 11805120, No. 12235020, and No. 12235003, Guangdong Major Project of Basic and Applied Basic

Research under Grants No. 2021B0301030006 and No. 11490562, the Continuous Basic Scientific Research Project No. WDJC-2019-13, and Research Grants Council (RGC) of Hong Kong (AoE/P-404/18 and GRF-17304720).

*Corresponding author.

xinxing@impcas.ac.cn

†Corresponding author.

sunlijie@sjtu.edu.cn

- [1] W. Heisenberg, *Z. Phys.* **77**, 1 (1932).
- [2] E. Wigner, *Phys. Rev.* **51**, 106 (1937).
- [3] J. C. Hardy and I. S. Towner, *Phys. Rev. C* **102**, 045501 (2020).
- [4] M. B. Bennett, C. Wrede, B. A. Brown, S. N. Liddick, D. Pérez-Loureiro, D. W. Bardayan *et al.*, *Phys. Rev. Lett.* **116**, 102502 (2016).
- [5] W. Trinder, E. Adelberger, Z. Janas, H. Keller, K. Krumbholz, V. Kunze *et al.*, *Phys. Lett. B* **349**, 267 (1995).
- [6] V. Tripathi, S. L. Tabor, A. Volya, S. N. Liddick, P. C. Bender, N. Larson, C. Prokop, S. Suchyta, P.-L. Tai, and J. M. VonMoss, *Phys. Rev. Lett.* **111**, 262501 (2013).
- [7] S. E. A. Orrigo, B. Rubio, Y. Fujita, B. Blank, W. Gelletly, J. Agramunt *et al.*, *Phys. Rev. Lett.* **112**, 222501 (2014).
- [8] J.-C. Thomas, L. Achouri, J. Äystö, R. Béraud, B. Blank, G. Canchel *et al.*, *Eur. Phys. J. A* **21**, 419 (2004).
- [9] B. Blank and M. Borge, *Prog. Part. Nucl. Phys.* **60**, 403 (2008).
- [10] B. Blank and M. Płoszajczak, *Rep. Prog. Phys.* **71**, 046301 (2008).
- [11] X. X. Xu, C. J. Lin, L. J. Sun, J. S. Wang, Y. H. Lam, J. Lee *et al.*, *Phys. Lett. B* **766**, 312 (2017).
- [12] J. Lee, X. X. Xu, K. Kaneko, Y. Sun, C. J. Lin, L. J. Sun *et al.* (RIBLL Collaboration), *Phys. Rev. Lett.* **125**, 192503 (2020).
- [13] R. Jahn, R. L. McGrath, D. M. Moltz, J. E. Reiff, X. J. Xu, J. Aysto, and J. Cerny, *Phys. Rev. C* **31**, 1576 (1985).
- [14] Y. Wang, D. Fang, K. Wang, X. Xu, L. Sun, P. Bao *et al.*, *Phys. Lett. B* **784**, 12 (2018).
- [15] G. T. Koldste, B. Blank, M. J. G. Borge, J. A. Briz, M. Carmona-Gallardo, L. M. Fraile *et al.*, *Phys. Rev. C* **89**, 064315 (2014).
- [16] L. Audirac, P. Ascher, B. Blank, C. Borcea, B. A. Brown, G. Canchel *et al.*, *Eur. Phys. J. A* **48**, 179 (2012).
- [17] H. O. U. Fynbo, M. J. G. Borge, L. Axelsson, J. Äystö, U. C. Bergmann, L. M. Fraile *et al.*, *Nucl. Phys.* **A677**, 38 (2000).
- [18] G. Z. Shi, J. J. Liu, Z. Y. Lin, H. F. Zhu, X. X. Xu, L. J. Sun *et al.*, *Phys. Rev. C* **103**, L061301 (2021).
- [19] P. F. Liang, L. J. Sun, J. Lee, S. Q. Hou, X. X. Xu, C. J. Lin *et al.* (RIBLL Collaboration), *Phys. Rev. C* **101**, 024305 (2020).
- [20] W. L. Zhan, J. W. Xia, H. W. Zhao, G. Q. Xiao, Y. J. Yuan, H. S. Xu *et al.*, *Nucl. Phys.* **A805**, 533c (2008).
- [21] L. J. Sun, X. X. Xu, C. J. Lin, J. S. Wang, D. Q. Fang, Z. H. Li *et al.*, *Nucl. Instrum. Methods Phys. Res., Sect. A* **804**, 1 (2015).
- [22] L. J. Sun, X. X. Xu, C. J. Lin, J. Lee, S. Q. Hou, C. X. Yuan *et al.* (RIBLL Collaboration), *Phys. Rev. C* **99**, 064312 (2019).

- [23] Z. Sun, W.-L. Zhan, Z.-Y. Guo, G. Xiao, and J.-X. Li, *Nucl. Instrum. Methods Phys. Res., Sect. A* **503**, 496 (2003).
- [24] C. G. Wu, H. Y. Wu, J. G. Li, D. W. Luo, Z. H. Li, H. Hua *et al.* (RIBLL Collaboration), *Phys. Rev. C* **104**, 044311 (2021).
- [25] H. Jian, Y. Gao, F. Dai, J. Liu, X. Xu, C. Yuan *et al.*, *Symmetry* **13**, 2278 (2021).
- [26] D. Pérez-Loureiro, C. Wrede, M. B. Bennett, S. N. Liddick, A. Bowe, B. A. Brown *et al.*, *Phys. Rev. C* **93**, 064320 (2016).
- [27] S. E. Koonin, *Phys. Lett. B* **70**, 43 (1977).
- [28] C. J. Lin, X. X. Xu, H. M. Jia, F. Yang, F. Jia, S. T. Zhang *et al.*, *Phys. Rev. C* **80**, 014310 (2009).
- [29] X. X. Xu, C. J. Lin, H. M. Jia, F. Yang, F. Jia, Z. D. Wu *et al.*, *Phys. Rev. C* **81**, 054317 (2010).
- [30] X. X. Xu, C. J. Lin, H. M. Jia, F. Yang, H. Q. Zhang, Z. H. Liu *et al.*, *Phys. Lett. B* **727**, 126 (2013).
- [31] J. Honkanen, M. D. Cable, R. F. Parry, S. H. Zhou, Z. Y. Zhou, and J. Cerny, *Phys. Lett. B* **133**, 146 (1983).
- [32] M. D. Cable, J. Honkanen, E. C. Schloemer, M. Ahmed, J. E. Reiff, Z. Y. Zhou, and J. Cerny, *Phys. Rev. C* **30**, 1276 (1984).
- [33] M. Wang, W. Huang, F. Kondev, G. Audi, and S. Naimi, *Chin. Phys. C* **45**, 030003 (2021).
- [34] K. Miernik, *Acta Phys. Pol. B* **44**, 483 (2013).
- [35] B. Singh, J. L. Rodriguez, S. S. M. Wong, and J. K. Tuli, *Nucl. Data Sheets* **84**, 487 (1998).
- [36] P. A. Zyla *et al.* (Particle Data Group), *Prog. Theor. Exp. Phys.* **2020**, 083C01 (2020).
- [37] N. Shimizu, T. Mizusaki, Y. Utsuno, and Y. Tsunoda, *Comput. Phys. Commun.* **244**, 372 (2019).
- [38] B. A. Brown and B. H. Wildenthal, *Annu. Rev. Nucl. Part. Sci.* **38**, 29 (1988).
- [39] B. A. Brown and W. A. Richter, *Phys. Rev. C* **74**, 034315 (2006).
- [40] W. E. Ormand and B. A. Brown, *Nucl. Phys. A* **491**, 1 (1989).
- [41] C. Yuan, C. Qi, F. Xu, T. Suzuki, and T. Otsuka, *Phys. Rev. C* **89**, 044327 (2014).
- [42] M. B. Bennett, C. Wrede, B. A. Brown, S. N. Liddick, D. Pérez-Loureiro, D. W. Bardayan *et al.*, *Phys. Rev. C* **93**, 064310 (2016).
- [43] W. M. MacDonald, *Phys. Rev.* **101**, 271 (1956).
- [44] M. Pfützner, M. Karny, L. V. Grigorenko, and K. Riisager, *Rev. Mod. Phys.* **84**, 567 (2012).
- [45] N. Michel, W. Nazarewicz, and M. Płoszajczak, *Phys. Rev. C* **82**, 044315 (2010).
- [46] E. Garrido, D. Fedorov, H. Fynbo, and A. Jensen, *Phys. Lett. B* **648**, 274 (2007).
- [47] D. Wang and W. A. Friedman, *Phys. Rev. C* **12**, 1684 (1975).
- [48] J. Le Bloas, L. Bonneau, P. Quentin, J. Bartel, and D. D. Strottman, *Phys. Rev. C* **86**, 034332 (2012).
- [49] S. G. Nilsson, *Mat. Fys. Medd. K. Dan. Vidensk. Selsk* **29**, 16 (1955), <http://cds.cern.ch/record/212345/files/p1.pdf>.
- [50] P. Möller, A. Sierk, T. Ichikawa, and H. Sagawa, *At. Data Nucl. Data Tables* **109–110**, 1 (2016).